

Design and Implementation of an Inertial Navigation System for Pedestrians Based on a Low-Cost MEMS IMU

Francesco Montorsi*, Fabrizio Pancaldi[†] and Giorgio M. Vitetta*

*Department of Engineering “Enzo Ferrari”, University of Modena and Reggio Emilia
Modena, Italy, Email: {francesco.montorsi, giorgio.vitetta}@unimore.it

[†]Department of Science and Methods for Engineering, University of Modena and Reggio Emilia
Modena, Italy, Email: fabrizio.pancaldi@unimore.it

Abstract—Inertial navigation systems for pedestrians are infrastructure-less and can achieve sub-meter accuracy in the short/medium period. However, when low-cost inertial measurement units (IMU) are employed for their implementation, they suffer from a slowly growing drift between the true pedestrian position and the corresponding estimated position. In this paper we illustrate a novel solution to mitigate such a drift by: a) using only accelerometer and gyroscope measurements (no magnetometers required); b) including the sensor error model parameters in the state vector of an extended Kalman filter; c) adopting a novel soft heuristic for foot stance detection and for zero-velocity updates. Experimental results evidence that our inertial-only navigation system can achieve similar or better performance with respect to pedestrian dead-reckoning systems presented in related studies, although the adopted IMU is less accurate than more expensive counterparts.

I. INTRODUCTION

In an *inertial navigation system* (INS) the position of a mobile agent is tracked by means of an *inertial measurement unit* (IMU) carried by the agent itself. IMU-based INSs can provide a *low-cost* and *infrastructure-less* solution to accurate indoor navigation in the short/medium term. Unluckily, in the medium/long term they usually suffer from a “drift” phenomenon [1], which originates from the noise and from any small bias in the accelerations and angular velocities sensed by the IMU.

Recently, substantial attention has been devoted to *pedestrian dead-reckoning* (PDR) INSs, where the prior knowledge of human walking patterns is exploited to reset, at least partially, the accumulated errors due to various error sources (e.g., the time-variant biases of IMUs). This approach has been first proposed in [2], where the periods during which the pedestrian’s foot is still on the ground are detected and exploited to introduce some corrections (the so-called *zero velocity updates* (ZUPTs)) in the tracking filter. Further advances have been developed in [1], [3]–[5]. In particular, in [1] and [3] an *extended Kalman filter* (EKF) processing IMU measurements exploits various heuristics to compensate for the drift due to time-variant biases and measurement noise. In [4] and [5], instead, additional measurements (from RFID devices) are adopted to mitigate the drift phenomenon.

In this manuscript, starting from the methods and the results illustrated in [1], [6], we develop a novel INS based only on a low-cost IMU which performs PDR employing an EKF. Unlike previous approaches, the proposed solution relies on:

- 1) Accelerometer and gyroscope measurements only (magnetometer sensors are often completely unreliable in indoor environments and other technologies for accurate localization are expensive).
- 2) A rigorous approach to the kinematic modelling of IMU measurements; this involves the use of a large EKF state vector, including both physical variables (e.g., agent position and heading) and quantities referring to the *sensor error models* (SEMs).
- 3) A new soft (rather than hard) heuristic for foot stance detection which increases the overall accuracy of the INS.

This manuscript is organized as follows. In Section II, the employed IMU and its calibration procedure are described. The proposed PDR-INS is illustrated in Section III, whereas its performance is assessed in Section IV. Finally, in Section V some conclusions are provided.

Notations: The *probability density function* (pdf) of a *random vector* (rv) \mathbf{R} evaluated at the point \mathbf{r} is denoted as $f(\mathbf{r})$; $\mathcal{N}(\mathbf{r}; \mathbf{m}, \Sigma)$ denotes the pdf of a Gaussian rv \mathbf{R} having mean \mathbf{m} and covariance matrix Σ , evaluated at the point \mathbf{r} ; $\|\mathbf{x}\|$ denotes the L^2 norm of vector \mathbf{x} ; the expressions $\{\mathbf{x}_i\}_{i=1}^k$ and $\mathbf{x}_{1:k}$ both denote the sequence $\mathbf{x}_1, \mathbf{x}_2, \dots, \mathbf{x}_k$. $g \triangleq 9.80665 \text{ m/s}^2$ denotes the gravitational acceleration; finally, \odot denotes the quaternion multiplication [7].

II. IMU DESCRIPTION AND CALIBRATION

In our PDR INS a mobile agent is equipped with a low-cost IMU, called RazorIMU [8] and fixed on one of his/her feet using shoes’ laces (e.g., see [1], [3]–[5]). It is important to note that the IMU-sensed quantities are expressed in *body* (or *sensor*) *frame*, i.e., they are referred to a right-handed coordinate frame centered on the IMU with axes parallel to the sensor sides; this frame is different from the so called *navigation frame*, which is a right-handed coordinate frame centered on some point of the navigation map and whose x

and y axes are parallel to Earth ground and z axis points away from Earth.

The RazorIMU is a programmable device equipped with 3-axis accelerometers, gyroscopes and magnetometers; our firmware outputs their measurements in “raw mode”, i.e., as integer numbers, so that a calibration procedure is required. The tri-axial accelerometer calibration procedure we adopted is similar to that described in [9], [10], but does not require any additional hardware (besides the IMU itself). It relies on the SEM (assuming a still sensor) [9], [10]

$$\mathbf{a}^m = \mathbf{G}_a \mathbf{a} + \mathbf{b}^a + \mathbf{n}^a \quad (1)$$

where $\mathbf{a}^m \in \mathbb{Z}^3$ is the vector of *measured* accelerations (in body frame), $\mathbf{a} \in \mathbb{R}^3$ is the vector of *true* accelerations (in body frame), $\mathbf{G}_a \in \mathbb{R}^{3 \times 3}$ is the *gain matrix* (diagonal if only scale factors are accounted for, or a generic invertible matrix if cross-couplings are also accounted for), $\mathbf{b}^a \in \mathbb{R}^3$ is the *bias* vector, in body frame, and $\mathbf{n}^a \in \mathbb{R}^3$ is the *noise* vector (in body frame) and is assumed to be *additive Gaussian noise* (AGN) with covariance matrix $\Sigma_a = \sigma_a^2 \mathbf{I}_3$. The calibration task for the accelerometer consists of estimating \mathbf{G}_a and \mathbf{b}^a on the basis of $N \cdot P$ measured vectors $\{\{\mathbf{a}_{i,p}^m\}_{i=1}^N\}_{p=1}^P$ (in our setup $N = 500$ and $P = 16$), referring to P unknown orientations of the still sensor (in the navigation frame). The optimal (in the *mean square error* sense) estimators $\hat{\mathbf{G}}_a$ and $\hat{\mathbf{b}}^a$ of the terms \mathbf{G}_a and \mathbf{b}^a appearing in (1) are given by

$$(\hat{\mathbf{G}}_a, \hat{\mathbf{b}}^a) = \arg \min_{(\tilde{\mathbf{G}}, \tilde{\mathbf{b}}) \in \mathcal{G} \times \mathcal{B}} \sum_{p=1}^P r_p(\tilde{\mathbf{G}}, \tilde{\mathbf{b}}, \bar{\mathbf{a}}_p^m) \quad (2)$$

where $\bar{\mathbf{a}}_p^m$ is the mean of the measurements $\{\mathbf{a}_{i,p}^m\}_{i=1}^N$ and

$$r_p(\tilde{\mathbf{G}}, \tilde{\mathbf{b}}, \bar{\mathbf{a}}_p^m) \triangleq \min_{\tilde{\mathbf{a}}_p \in \mathcal{A}} \|\tilde{\mathbf{G}} \tilde{\mathbf{a}}_p + \tilde{\mathbf{b}} - \bar{\mathbf{a}}_p^m\|^2 \quad (3)$$

Once calibration is completed, the true acceleration vector may be estimated as

$$\hat{\mathbf{a}} = \hat{\mathbf{G}}_a^{-1} (\mathbf{a}^m - \hat{\mathbf{b}}^a). \quad (4)$$

Regarding the gyroscopes, a SEM similar to (1), i.e.,

$$\boldsymbol{\omega}^m = \mathbf{G}_\omega \boldsymbol{\omega} + \mathbf{b}^\omega + \mathbf{n}^\omega \quad (5)$$

has been exploited to devise our calibration procedure; here $\boldsymbol{\omega}^m \in \mathbb{Z}^3$ is the vector of measured angular velocities (in body frame), $\boldsymbol{\omega} \in \mathbb{R}^3$ is the vector of true angular velocities (in body frame), $\mathbf{G}_\omega \in \mathbb{R}^{3 \times 3}$ is the gain matrix (diagonal if only scale factors are accounted for, or a generic invertible matrix if cross-couplings are also accounted for), $\mathbf{b}^\omega \in \mathbb{R}^3$ is the bias vector (in body frame), and $\mathbf{n}^\omega \in \mathbb{R}^3$ is the noise vector (in body frame) and is assumed to be AGN with covariance matrix $\Sigma_\omega = \sigma_\omega^2 \mathbf{I}_3$. Similarly to (4), the true vector $\boldsymbol{\omega}$ is estimated as

$$\hat{\boldsymbol{\omega}} = \hat{\mathbf{G}}_\omega^{-1} (\boldsymbol{\omega}^m - \hat{\mathbf{b}}^\omega) \quad (6)$$

where $\hat{\mathbf{G}}_\omega$ and $\hat{\mathbf{b}}^\omega$ denote the estimated bias vector and gain matrix of the gyroscope, respectively. However, unlike accelerometer calibration, calibration of gyroscopes requires an

expensive dedicated hardware platform, so that $\hat{\mathbf{b}}^\omega = 0$ and the value provided in the gyroscope datasheet [8] for $\hat{\mathbf{G}}_\omega$ have been adopted.

III. THE PDR INS

Our INS performs similarly to some other navigation systems described in the technical literature (e.g., see [1]), but is based on a different approach and, in particular, on a set of rigorous kinematic equations relating the quantities sensed by the IMU with its orientation and 3D position. After describing the structure of the state vector, the dynamic models and the measurement models, we describe the use of an EKF for estimating the posterior distribution of the state vector. Finally, we focus on a soft algorithm for foot stance detection.

A. State Vector

In our INS the state vector \mathbf{x}_k of the mobile agent wearing the IMU is defined as

$$\mathbf{x}_k \triangleq [\mathbf{p}_k, \mathbf{v}_k, \mathbf{a}_k, q_k^{n \triangleright b}, \mathbf{a}_k^b, \boldsymbol{\omega}_k^{b, b \triangleright n}, \mathbf{b}_k^a, \mathbf{b}_k^\omega]^T \in \mathbb{R}^D \quad (7)$$

where k is the time-index of the discrete-time tracking filter for navigation, $\mathbf{p}_k \in \mathbb{R}^3$, $\mathbf{v}_k \in \mathbb{R}^3$ and $\mathbf{a}_k \in \mathbb{R}^3$ are the position, the velocity and the acceleration of the IMU sensor, measured in m, m/s and m/s², respectively; $q_k^{n \triangleright b} \in \mathbb{H}_1$ is a (random) *quaternion* representing the transformation which produces, given a vector in navigation coordinates, a vector in body coordinates [7]; \mathbf{a}_k^b and $\boldsymbol{\omega}_k^{b, b \triangleright n} \in \mathbb{R}^3$ are the acceleration (in body frame) and the angular velocity (from body to navigation frame, resolved in body coordinate frame [6]), measured in m/s² and rad/s, respectively; $\mathbf{b}_k^a \in \mathbb{R}^3$ and $\mathbf{b}_k^\omega \in \mathbb{R}^3$ are the bias vectors of the accelerometer and of the gyroscope, expressed in body coordinate frame and measured in m/s² and rad/s, respectively; finally, $D = 25$ is the size of \mathbf{x}_k .

Note that: a) \mathbf{a}_k^b and $\boldsymbol{\omega}_k^{b, b \triangleright n}$ are the (noisy) observable variables; b) all the other variables can be *pseudo-observed* to enhance the system stability whenever the foot is (approximately) still; c) \mathbf{b}_k^a and \mathbf{b}_k^ω represent “fine” bias vectors, and play a complementary role with respect to $\hat{\mathbf{b}}^a$ and $\hat{\mathbf{b}}^\omega$, respectively, which account for time-variant and turn-on dependent biases; d) the vector \mathbf{x}_k (7) has an heterogeneous structure, since it consists of quantities of interest for the end-user of the INS (namely, \mathbf{p}_k and \mathbf{v}_k), quantities relating \mathbf{p}_k and \mathbf{v}_k to the sensor outputs (namely, \mathbf{a}_k , $q_k^{n \triangleright b}$, \mathbf{a}_k^b , $\boldsymbol{\omega}_k^{b, b \triangleright n}$) and quantities related to the SEMs of accelerometers and gyroscopes (\mathbf{b}_k^a and \mathbf{b}_k^ω , respectively); e) including the IMU-sensed quantities (\mathbf{a}_k^b , $\boldsymbol{\omega}_k^{b, b \triangleright n}$) in \mathbf{x}_k is important since impulsive noise (due to hardware instability of low-cost sensors) may affect the IMU output and an accurate dynamic modelling of $(k+1)$ -th step sensor orientation ($q_{k+1}^{n \triangleright b}$) requires the knowledge of the k -th step angular velocity ($\boldsymbol{\omega}_k^{b, b \triangleright n}$).

B. Dynamic and Measurement Models

The dynamic models adopted for the elements of \mathbf{x}_k (7) can be summarised as follows. The Taylor-expansion models (e.g., see [6], [11, Sec. 4.3])

$$\mathbf{p}_{k+1} = \mathbf{p}_k + \mathbf{v}_k \cdot T_s + \frac{1}{2} \mathbf{a}_k \cdot T_s^2 + \mathbf{n}_{p,k} \quad (8)$$

and

$$\mathbf{v}_{k+1} = \mathbf{v}_k + \mathbf{a}_k \cdot T_s + \mathbf{n}_{v,k} \quad (9)$$

have been employed for the vectors \mathbf{p}_k and \mathbf{v}_k , respectively; here T_s denotes the sampling period of the INS (1/100 Hz in our case) and the vectors $\mathbf{n}_{p,k}$ and $\mathbf{n}_{v,k}$ are AGN terms affecting \mathbf{p}_k and \mathbf{v}_k , respectively. The model

$$\mathbf{a}_{k+1} = R^T(q_k^{n \triangleright b}) \mathbf{a}_k^b + \mathbf{g} + \mathbf{n}_{a,k} \quad (10)$$

has been used for \mathbf{a}_k , where $R(q_k^{n \triangleright b})$ is the rotation matrix associated with the quaternion $q_k^{n \triangleright b}$ (and thus representing the transformation from navigation to body frame), $\mathbf{g} \triangleq [0, 0, -g]^T$ is the gravity vector in the navigation frame and $\mathbf{n}_{a,k}$ is AGN.

A further model relates the orientation of the sensor (represented by $q_k^{n \triangleright b}$) to the angular velocity $\omega_k^{b, b \triangleright n}$ and is given by (e.g., see [6, Eq. (4.11), Eq. (4.20d)] and [7, Sec. 11.5])

$$q_{k+1}^{n \triangleright b} = \exp\left(-\frac{T}{2} \omega_k^{b, b \triangleright n}\right) \odot q_k^{n \triangleright b} + \mathbf{n}_{q,k} \quad (11)$$

where $\mathbf{n}_{q,k}$ is AGN.

Finally, the simple “random walk” models

$$\mathbf{a}_{k+1}^b = \mathbf{a}_k^b + \mathbf{n}_{a,k} \quad (12)$$

$$\omega_{k+1}^{b, b \triangleright n} = \omega_k^{b, b \triangleright n} + \mathbf{n}_{\omega,k} \quad (13)$$

$$\mathbf{b}_{k+1}^a = \mathbf{b}_k^a + \mathbf{n}_{b^a,k} \quad (14)$$

$$\mathbf{b}_{k+1}^\omega = \mathbf{b}_k^\omega + \mathbf{n}_{b^\omega,k} \quad (15)$$

have been selected for the filtered states \mathbf{a}_k^b and $\omega_k^{b, b \triangleright n}$, and for the sensor biases \mathbf{b}_k^a and \mathbf{b}_k^ω , where the $\{\mathbf{n}_{\cdot,k}\}$ terms denote AGN contributions.

Regarding measurements models, simple linear relations involving only quantities in the body frame may be adopted, thanks to the structure chosen for \mathbf{x}_k (7):

$$\mathbf{z}_k^f = \mathbf{a}_k^b + \mathbf{b}_k^a + \mathbf{m}_{a,k} \quad (16)$$

$$\mathbf{z}_k^\omega = \omega_k^{b, b \triangleright n} + \mathbf{b}_k^\omega + \mathbf{m}_{\omega,k} \quad (17)$$

Here $\mathbf{z}_k^f = \hat{\mathbf{a}}$ (see (4)) and $\mathbf{z}_k^\omega = \hat{\omega}$ (see (6)) denote the *calibrated* force and angular velocity measurements provided by the IMU and the vectors $\mathbf{m}_{a,k}$, $\mathbf{m}_{\omega,k}$ represent the AGN terms affecting the measurements.

The *dynamic* models (8)-(15) can be summarised as

$$f(\mathbf{x}_{k+1}|\mathbf{x}_k) = \mathcal{N}(\mathbf{x}_{k+1}; \mathbf{q}(\mathbf{x}_k), \mathbf{Q}) \quad (18)$$

whereas the *measurement* models (16)-(17) can be summarised as

$$f(\mathbf{z}_k|\mathbf{x}_k) = \mathcal{N}(\mathbf{z}_k; \mathbf{r}(\mathbf{x}_k), \mathbf{R}) \quad (19)$$

where $\mathbf{z}_k \triangleq [\mathbf{z}_k^f, \mathbf{z}_k^\omega]^T \in \mathbb{R}^M$ (with $M = 6$), the vector functions $\mathbf{q}(\cdot)$ and $\mathbf{r}(\cdot)$ are defined by (8)-(15) and by (16)-(17), respectively, and \mathbf{Q} and \mathbf{R} are $D \times D$ and $M \times M$ diagonal covariance matrices for the AGN terms. Regarding these matrices, it is worth mentioning that a) they may have a strong impact on the EKF stability and b) the choice of their diagonal values can be based, in practice, on some careful tuning procedure (involving $D + M = 31$ parameters).

C. The EKF

The goal of the INS is the sequential estimation of the hidden state vector \mathbf{x}_k representing the mobile agent given the sequence of IMU measurements $\{\mathbf{z}_{0:k}\}$, i.e., the sequential estimation of the posterior pdf $f(\mathbf{x}_k|\mathbf{z}_{0:k})$. Since our dynamic model is non-linear (see (10) and (11)), a non-linear filter, such as an EKF, needs to be employed to solve this problem. It is important to mention that: a) the EKF alternates a *prediction step* with an *update step*; b) it estimates the first two moments of the posterior pdf $f(\mathbf{x}_k|\mathbf{z}_{0:k})$, namely, the mean state vector $\hat{\mathbf{x}}_k^{\text{EKF}}$ and the state vector covariance matrix $\hat{\mathbf{P}}_k^{\text{EKF}}$, in a recursive fashion. In particular, given $\hat{\mathbf{x}}_k^{\text{EKF}}$ and $\hat{\mathbf{P}}_k^{\text{EKF}}$, the EKF estimates (*prediction step*) [12]

$$\hat{\mathbf{x}}_{k+1|k}^{\text{EKF}} = \mathbf{q}(\hat{\mathbf{x}}_k^{\text{EKF}}) \quad \hat{\mathbf{P}}_{k+1|k}^{\text{EKF}} = \mathbf{J}_k^q \hat{\mathbf{P}}_k^{\text{EKF}} (\mathbf{J}_k^q)^T + \mathbf{Q}$$

where $\hat{\mathbf{x}}_{k+1|k}^{\text{EKF}}$ and $\hat{\mathbf{P}}_{k+1|k}^{\text{EKF}}$ denote the $(k+1)$ -th state mean and covariance, respectively, which can be predicted on the basis of the information available at the k -th step; here $\mathbf{J}_k^q \triangleq \left. \frac{\partial \mathbf{q}(\mathbf{x})}{\partial \mathbf{x}} \right|_{\hat{\mathbf{x}}_k}$ is the $D \times D$ Jacobian matrix¹ for our (non-linear) dynamic model. Then, the EKF evaluates (*update step*) [12]:

$$\begin{aligned} \mathbf{s}_{k+1|k} &= \mathbf{z}_k - \mathbf{r}(\hat{\mathbf{x}}_{k+1|k}^{\text{EKF}}) \\ \mathbf{S}_{k+1|k} &= \mathbf{J}_k^r \hat{\mathbf{P}}_{k+1|k}^{\text{EKF}} (\mathbf{J}_k^r)^T + \mathbf{R} \\ \mathbf{K}_{k+1|k} &= \hat{\mathbf{P}}_{k+1|k}^{\text{EKF}} (\mathbf{J}_k^r)^T \mathbf{S}_{k+1|k}^{-1} \\ \hat{\mathbf{x}}_{k+1}^{\text{EKF}} &= \hat{\mathbf{x}}_{k+1|k}^{\text{EKF}} + \mathbf{K}_{k+1|k} \mathbf{s}_{k+1|k} \\ \hat{\mathbf{P}}_{k+1}^{\text{EKF}} &= (\mathbf{I} - \mathbf{K}_{k+1|k} \mathbf{J}_k^r) \hat{\mathbf{P}}_{k+1|k}^{\text{EKF}} \end{aligned}$$

where $\mathbf{r}_{k+1|k}$ is the innovation residual and $\mathbf{S}_{k+1|k}$ its estimated covariance matrix, $\mathbf{K}_{k+1|k}$ is the Kalman gain, $\hat{\mathbf{x}}_{k+1}^{\text{EKF}}$ is the new estimate of the state vector mean and $\hat{\mathbf{P}}_{k+1}^{\text{EKF}}$ is its estimated covariance matrix; moreover, $\mathbf{J}_k^r \triangleq \left. \frac{\partial \mathbf{r}(\mathbf{x})}{\partial \mathbf{x}} \right|_{\hat{\mathbf{x}}_{k+1|k}}$ is the $M \times D$ Jacobian matrix for the measurement model.

It is worth noting that: a) in any EKF, at the end of the k -th iteration only the quantities $\hat{\mathbf{x}}_k^{\text{EKF}}$ and $\hat{\mathbf{P}}_k^{\text{EKF}}$ need to be saved and this substantially simplifies the INS implementation; b) given these quantities, the posterior distribution $f(\mathbf{x}_k|\mathbf{z}_{0:k})$ is estimated by the EKF as $\mathcal{N}(\mathbf{x}_k; \hat{\mathbf{x}}_k^{\text{EKF}}, \hat{\mathbf{P}}_k^{\text{EKF}})$; c) the initialisation of the INS represent a critical task, since initial errors cannot be mitigated by the EKF. As far as the last point is concerned, $\hat{\mathbf{P}}_0^{\text{EKF}} = \mathbf{Q}$ has been selected for the initial covariance matrix, whereas the initial state vector $\hat{\mathbf{x}}_0^{\text{EKF}}$ has been estimated assuming the foot still in a known position; unfortunately, further details cannot be provided for space limitations.

D. Foot Stance Detection

Even if the EKF illustrated in the previous Paragraph includes the sensor biases \mathbf{b}_k^a and \mathbf{b}_k^ω in \mathbf{x}_k , due to the lack of robust models and, in particular, to the lack of bias observations, the tracking of such quantities mitigates but

¹This matrix cannot be put in a simple analytical form, so that its evaluation requires use of computer algebra systems.

does not completely compensate for sensor inaccuracies. In practice, the residual biases may quickly disrupt the INS tracking since their effects accumulate over time. The effects of these error sources can be mitigated exploiting some a priori knowledge about the typical human walking pattern and, in particular, the fact at the end of each step the foot lies approximately still on the ground for a short period (typically, 0.1 – 0.2 s); during such a period, the value of most of the elements of \mathbf{x}_k are known a priori and the EKF state can be adjusted accordingly. In practice, the EKF can be provided with some “pseudo-measurements”, usually known as ZUPTs [2], whenever a detection algorithm, processing the IMU measurements in parallel to the EKF, detects a “foot still event”. In our work, a foot stance detection algorithm inspired by [1, Sec. II.C] has been used. This algorithm evaluates four logical “condition signals” $\{C_i^1, C_i^2, C_i^3, C_i^4\}$ associated with the IMU measurements \mathbf{z}_k and generated as

$$\begin{aligned} C_i^1 &\triangleq \begin{cases} 1 & \gamma_{a,\min} < \|\mathbf{z}_i^f\| < \gamma_{a,\max} \\ 0 & \text{otherwise} \end{cases} \\ C_i^2 &\triangleq \begin{cases} 1 & \sigma(\mathbf{z}_{i-S:i+S}^f) < \sigma_{a,\max} \\ 0 & \text{otherwise} \end{cases} \\ C_i^3 &\triangleq \begin{cases} 1 & \|\mathbf{z}_i^\omega\| < \gamma_{\omega,\max} \\ 0 & \text{otherwise} \end{cases} \\ C_i^4 &\triangleq \begin{cases} 1 & \sigma(\mathbf{z}_{i-S:i+S}^\omega) < \sigma_{\omega,\max} \\ 0 & \text{otherwise} \end{cases} \end{aligned}$$

for $i \in \{k - F, \dots, k + F\}$, where $\sigma(\mathbf{x}_1, \mathbf{x}_2, \dots, \mathbf{x}_N)$ denotes the standard deviation of the magnitude of the vectors $\{\mathbf{x}_1, \mathbf{x}_2, \dots, \mathbf{x}_N\}$, F is the size of the windows used for step detection, S is the size of the window used for the computation of $\sigma(\cdot)$, and $\gamma_{a,\max}$, $\sigma_{a,\max}$, $\gamma_{\omega,\max}$ and $\sigma_{\omega,\max}$ represent proper thresholds. An *hard* detection algorithm based on the condition signals defined above has been proposed in [1, Sec. II.C]; it decides that the foot is “still”, during the k -th time step, if $\sum_{j=k-F}^{k+F} C_j^1 C_j^2 C_j^3 > \frac{F}{2}$. Here, we propose to use a *soft* variant whose output is the *soft foot still* (SFS) signal

$$\text{SFS}_k \triangleq \frac{1}{F} \sum_{i=k-F}^{k+F} C_i^1 C_i^2 C_i^3 C_i^4$$

which ranges, for the k -th time step, from zero (moving foot) to one (the foot is very likely to be still on the ground). Then, whenever $\text{SFS}_k > \gamma_{\text{SFS}}$ ($\gamma_{\text{SFS}} \in [0; 1]$ is a fixed threshold), a “foot still event” begins and the EKF is fed with the pseudo-measurements

$$[\hat{\mathbf{p}}_s^{\text{EKF}}]_{1:2} = \mathbf{z}^{xy} = [\mathbf{p}_k]_{1:2} + \mathbf{m}_{xy,k} \quad (20)$$

$$0 = z^z = [\mathbf{p}_k]_3 + m_{z,k} \quad (21)$$

$$\mathbf{0} = \mathbf{z}^v = \mathbf{v}_k + \mathbf{m}_{v,k} \quad (22)$$

$$\mathbf{0} = \mathbf{z}^a = \mathbf{a}_k + \mathbf{m}_{a,k} \quad (23)$$

$$-\mathbf{g} = \mathbf{z}^a = R^T (q_k^{n \triangleright b}) \mathbf{a}_k^b + \mathbf{m}_{a^b,k} \quad (24)$$

$$\|\mathbf{g}\| = \mathbf{z}^a = \|\mathbf{a}_k^b\| + m_{a^b,k} \quad (25)$$

$$\mathbf{0} = \mathbf{z}^\omega = \boldsymbol{\omega}_k^{b, b \triangleright n} + \mathbf{m}_{\omega,k} \quad (26)$$

$$\hat{\mathbf{a}} = \mathbf{z}_k^{b^a} = \mathbf{b}_k^a - R(q_k^{n \triangleright b}) \mathbf{g} + \mathbf{m}_{b^a,k} \quad (27)$$

$$\hat{\boldsymbol{\omega}} = \mathbf{z}_k^{b^\omega} = \mathbf{b}_k^\omega + \mathbf{m}_{b^\omega,k} \quad (28)$$

where s is the time step corresponding to the beginning of the current “foot still event” (so that $\hat{\mathbf{p}}_s^{\text{EKF}}$ represents the position where the foot is still) and the vectors $\{\mathbf{m}_{\cdot,k}\}$ denote the AGN terms of the pseudo-measurement models. To avoid discontinuities in the tracked path, the variance of these noise terms is modulated in a *soft* way on the basis of the SFS_k signal. In practice, the soft ZUPT pseudo-measurement model

$$f(\mathbf{z}_k^p | \mathbf{x}_k) = \mathcal{N}(\mathbf{z}_k^p; \mathbf{r}^p(\mathbf{x}_k), [1 + K^p(1 - \text{SFS}_k)] \mathbf{R}^p) \quad (29)$$

is adopted where $\mathbf{z}_k^p \triangleq [z_k^{xy}, z_k^z, \mathbf{z}_k^v, \dots, \mathbf{z}_k^{b^\omega}]^T \in \mathbb{R}^{M^p}$ (with $M^p = 20$); \mathbf{R}^p is the diagonal covariance matrix collecting all variance values of the $\{\mathbf{m}_{\cdot,k}\}$ terms; the vector function $\mathbf{r}^p(\cdot)$ can be easily derived from (20)-(28); $\mathbf{J}_k^{r^p} \triangleq \frac{\partial \mathbf{r}^p(\mathbf{x})}{\partial \mathbf{x}} \Big|_{\hat{\mathbf{x}}_{k+1|k}}$ is the $M^p \times D$ Jacobian matrix associated with the measurement model (29) and K^p is a parameter introduced to modulate the variance of ZUPT pseudo-measurements. Note that the value of K^p , the higher will be the variances associated to \mathbf{z}_k^p pseudo-measurement when $\text{SFS}_k = \gamma_{\text{SFS}}$; then, as SFS_k goes from γ_{SFS} to 1, the variances associated to \mathbf{z}_k^p decrease smoothly to the values collected in \mathbf{R}^p . This approach ensures that the tracked state vector $\hat{\mathbf{x}}_k^{\text{EKF}}$ smoothly transitions to the “reset” values defined by (20)-(28), when ZUPTs are injected in the EKF.

Finally, it is worth noting that the pseudo-measurements (20), (21), (22), (27) and (28) allow to “observe” otherwise unobservable state vector components and thus to “reset” errors they might contain.

IV. INDOOR NAVIGATION TESTS

An experimental campaign has been carried out to acquire various sets of measurements generated by an agent equipped with the IMU described in Section II and repeating the same test trajectory $N_{\text{rep}} = 10$ times in an indoor environment. These measurement sets have been stored on a notebook and then processed offline. The test trajectory contains long straight lines, 90 deg turns, short and long stops (e.g., to turn on/off lights, to open/close doors, etc); the initial and final positions coincide and the *total travelled distance* (TTD) L_{TTD} associated to such test walk is $L_{\text{TTD}} \simeq 300$ m.

An example of the resulting INS-estimated agent path² is shown in Fig. 1. It is easy to recognize that the “drift” phenomenon mentioned in Section I is present, although in a very limited amount (specially considering the many loops walked in the same verse by the agent).

To quantify the performance of the INS usually the quantity $\epsilon_{\text{TTD}} \triangleq \frac{1}{L_{\text{TTD}}} \|\hat{\mathbf{p}}_0^{\text{EKF}} - \hat{\mathbf{p}}_{N_s}^{\text{EKF}}\|$ is exploited [1], where N_s is the last time step in the recorded measurement set; of course,

²Note that the values of the parameters introduced throughout the paper and used to produce such results have been properly *tuned* by means of an automated search procedure, but the resulting values cannot be shown for space limitations; see [13] for more details.

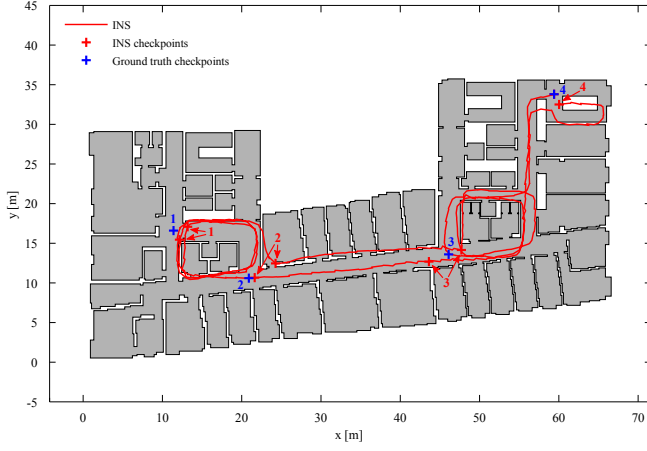


Figure 1. The agent trajectory estimated by the INS described in Section III for a specific repetition. The checkpoints approximating the ground truth are indicated by blue crosses; the corresponding points estimated by the INS are indicated by red crosses.

for a closed test path and an ideal INS, $\epsilon_{\text{TDD}} = 0$. In our tests, for the N_{rep} repetitions of the test walk, the ϵ_{TDD} figure of merit was $\{1.4, 0.5, 4.7, 1.5, 7.2, 1.6, 8.8, 10.1, 10.4, 12.1\}$; these results can be compared with those obtained in [1, Table II]; in such contribution, when the magnetometer is not employed, the reported range for ϵ_{TDD} is 2 – 10. These results show that our INS achieves similar performance to that of [1], despite the key difference that in [1] the Xsens MTi IMU has been employed. Such an IMU has higher accuracy (and higher costs) than the RazorIMU; to quantify such a difference, the noise of the IMU sensors can be modelled analysing, by means of the Allan variance method, long sequences of sensor outputs acquired while the sensor is still. In our case, 24h of RazorIMU accelerometer and gyroscope data, acquired at the sampling frequency $f_s = 100$ Hz have been recorded and analysed; the results, in terms of the standard N and B coefficients representing *acceleration/angular velocity random walk* (ARW) and *bias instability* (BI) noise contributions, are listed in Table I, together with the results reported in [14, Table III] for the Xsens MTi IMU. The comparison between the two IMUs shows that: a) the Xsens MTi has better matching among the sensors mounted on the x , y and z axis; b) the Xsens MTi IMU offers much better accelerometer performance. Moreover, it is important to note that the RazorIMU calibration has been carried out at a fixed temperature while the Xsens IMUs employ temperature-dependent calibration factors.

In summary, the values of ϵ_{TDD} characterizing our INS are comparable to the values reported in [1, Table II] (when the magnetometer sensors are not used) although we employed an IMU with worse noise and bias characteristics (of course, our IMU is also cheaper and thus lowers system costs).

V. CONCLUSIONS

In this manuscript, a novel INS has been derived integrating exact kinematic models, SEM in the EKF state vector and a novel *soft* heuristic to detect foot steps. Our experimental tests

	IMU	ARW/BI coefficient	Unit
gyro	RazorIMU	$N = [5.2, 12.1, 5.6] \cdot 10^{-3}$	$(^\circ/\text{s})/\sqrt{\text{Hz}}$
		$B = [3, 18, 4.4] \cdot 10^{-3}$	$^\circ/\text{s}$
	Xsens MTi	$N = [45, 41, 36] \cdot 10^{-3}$	$(^\circ/\text{s})/\sqrt{\text{Hz}}$
		$B = [7, 7, 5] \cdot 10^{-3}$	$^\circ/\text{s}$
accel.	RazorIMU	$N = [5.5, 5.1, 7.6] \cdot 10^{-3}$	$(\text{m}/\text{s}^2)/\sqrt{\text{Hz}}$
		$B = [609, 590, 732] \cdot 10^{-6}$	m/s^2
	Xsens MTi	$N = [900, 950, 850] \cdot 10^{-6}$	$(\text{m}/\text{s}^2)/\sqrt{\text{Hz}}$
		$B = [230, 270, 290] \cdot 10^{-6}$	m/s^2

Table I
COMPARISON BETWEEN THE RAZORIMU AND THE XSSENS MTi IMU.

have evidenced that: a) a good accuracy can be achieved in tracking a mobile agent on the short/medium period; b) our INS performs similarly to other state-of-art INS PDR solutions but uses a lower-cost IMU and does not employ magnetometers which are often unreliable in indoor environments. Future work will focus the integration of map-awareness and radio measurements in the proposed INS in order to further improve robustness and long-term accuracy.

REFERENCES

- [1] A. R. Jiménez, F. Seco, J. C. Prieto, and J. Guevara Rosas, "Indoor pedestrian navigation using an INS/EKF framework for yaw drift reduction and a foot-mounted IMU," in *Workshop on Positioning Navigation and Communication*, Dresden, 2010, pp. 135–143.
- [2] E. Foxlin, "Pedestrian tracking with shoe-mounted inertial sensors," *IEEE Comput. Graph. Appl.*, vol. 25, no. 6, pp. 38–46, Nov. 2005.
- [3] A. R. Jiménez, F. Seco, F. Zampella, J. C. Prieto, and J. Guevara Rosas, "Improved Heuristic Drift Elimination (iHDE) for pedestrian navigation in complex buildings," in *Int. Conf. on Indoor Positioning and Indoor Navigation*, Guimaraes, 2011, pp. 1–8.
- [4] A. R. Jiménez, F. Seco, J. C. Prieto, and J. Guevara Rosas, "Accurate Pedestrian Indoor Navigation by Tightly Coupling Foot-Mounted IMU and RFID Measurements," *IEEE Trans. Instrum. Meas.*, vol. 61, no. 1, pp. 178–189, Jan. 2012.
- [5] B. Krach and P. Roberston, "Cascaded estimation architecture for integration of foot-mounted inertial sensors," in *IEEE/ION Position, Location and Navigation Symp.*, Monterey, CA, 2008, pp. 112–119.
- [6] J. Hol, "Pose Estimation and Calibration Algorithms for Vision and Inertial Sensors," Ph.D. dissertation, Linköping University, 2008.
- [7] J. B. Kuipers, *Quaternions and Rotation Sequences: A Primer with Applications to Orbits, Aerospace, and Virtual Reality*. Princeton University Press, 1999.
- [8] "9 Degrees of Freedom Razor IMU SEN-10736 schematic and sensors' datasheets," Available online at <http://www.sparkfun.com>.
- [9] P. Batista, C. Silvestre, P. Oliveira, and B. Cardeira, "Accelerometer Calibration and Dynamic Bias and Gravity Estimation: Analysis, Design, and Experimental Evaluation," *IEEE Trans. Control Syst. Technol.*, vol. 19, no. 5, pp. 1128–1137, Sep. 2011.
- [10] M. Sipos, P. Paces, J. Rohac, and P. Novacek, "Analyses of Triaxial Accelerometer Calibration Algorithms," *IEEE Sensors J.*, vol. 12, no. 5, pp. 1157–1165, May 2012.
- [11] X. Rong Li and V. Jilkov, "Survey of maneuvering target tracking. Part I. Dynamic models," *IEEE Trans. Aerosp. and Electron. Syst.*, vol. 39, no. 4, pp. 1333–1364, Oct. 2003.
- [12] R. E. Kalman, "A New Approach to Linear Filtering and Prediction Problems," *Trans. of the ASME – J. of Basic Eng.*, vol. 82, no. Series D, pp. 35–45, 1960.
- [13] F. Montorsi, "Localization and Tracking for Indoor Environments," Ph.D. dissertation, University of Modena and Reggio Emilia, 2013.
- [14] F. Hoffinger, J. Muller, M. Tork, L. Reindl, and W. Burgard, "A wireless micro inertial measurement unit (IMU)," in *IEEE Int. Instrumentation and Measurement Technology Conf.*, Graz, 2012, pp. 2578–2583.